

Nuclear Envelope and Chromatin Compositional Differences Comparing Undifferentiated and Retinoic Acid- and Phorbol Ester-Treated HL-60 Cells

Ada L. Olins,* Harald Herrmann,† Peter Lichter,‡ Martin Kratzmeier,§
Detlef Doenecke,|| and Donald E. Olins*¹

**Foundation for Blood Research, P.O. Box 190, 69 U.S. Route One, Scarborough, Maine 04070-0190;* †*Division of Cell Biology and ‡Organization of Complex Genomes, German Cancer Research Center, Im Neuenheimer Feld 280, Heidelberg, Germany;* §*Agilent Technologies GmbH, Hewlett-Packard-Str. 8, Waldbronn, Germany; and ||Institute for Biochemistry and Molecular Cell Biology, University of Göttingen, Humboldtallee 23, Göttingen, Germany*

The human leukemic cell line (HL-60) can be induced to differentiate *in vitro* to granulocytic form with retinoic acid (RA), or to monocytic/macrophage form with phorbol ester (TPA). The granulocytic form acquires nuclear lobulation, nuclear envelope-limited chromatin sheets (ELCS), and cytoskeletal polarization, none of which are acquired following treatment with TPA. Immunoblotting analyses and capillary zone electrophoresis demonstrated that following RA treatment: lamins A/C and B1, and vimentin decreased to negligible amounts; LAP2 β , lamin B2 and emerin remained essentially unchanged; lamin B receptor (LBR) increased markedly; histone subtypes H1.4 and 1.5 exhibited dephosphorylation. Following TPA treatment: lamins A/C and B1, B2 and vimentin increased in amount; LAP2 β and emerin remained essentially unchanged; LBR increased markedly; histone subtypes H1.4 and 1.5 exhibited dephosphorylation. Emerin, which was cytoplasmic in undifferentiated or granulocytic cells, localized into the nuclear envelope following TPA. Normal human granulocytes revealed compositional differences compared to granulocytic forms of HL-60, namely increased vimentin and appearance of histone subtype H1.3. A working hypothesis for nuclear lobulation postulates a combination of: increased nuclear envelope deformability due to lamins A/C and B1 deficiency; an increase in nuclear surface area/volume; an increase in chromatin-nuclear envelope interactions. © 2001 Academic Press

Key Words: nuclear envelope; histone H1; HL-60; retinoic acid; granulocytes.

INTRODUCTION

The human myeloid leukemia cell line (HL-60) is widely investigated as a model for inducible cell differ-

entiation [1–3]: all-*trans* retinoic acid (RA) or dimethyl sulfoxide (DMSO) stimulates granulocytic differentiation; 1,25-dihydroxy vitamin D₃, sodium butyrate, or 12-O-tetradecanoylphorbol-13-acetate (TPA) promotes monocytic/macrophage differentiation. RA- or DMSO-differentiated HL-60 cells exhibit similarities and differences with normal blood neutrophils [1–4]. In parallel with normal neutrophils, RA- or DMSO-differentiated HL-60 exhibit: nuclear lobulation; nitro blue tetrazolium (NBT) reduction by superoxide anions; enhanced expression of the cell surface antigen CD11b; and phagocytotic capability. Also, in parallel to normal neutrophils, granulocytic (as well as monocytic/macrophage) differentiated HL-60 cells eventually die by apoptosis [5–7]. Some of the differences observed between RA- or DMSO-induced granulocytes and normal neutrophils include: a higher proportion of immature granulocytic nuclear morphologies after RA or DMSO treatment, compared to peripheral blood neutrophils; and the inability of chemically induced granulocytes to sort certain granule proteins [8].

Previous studies from this laboratory [9, 10] have focused upon nuclear and cytoskeletal changes that occur during chemically induced differentiation of HL-60, at both the biochemical and the microscopic levels. The initial study [9] explored mechanisms of nuclear lobulation in response to RA. Unexpectedly, in addition to lobulation, extensive extrusions of the nuclear envelope were also induced in over 80% of the granulocytic cells. These nuclear envelope-limited chromatin sheets (ELCS) consist of a single layer of close-packed 20- to 30-nm chromatin fibers, bounded on both sides by the inner and outer membranes of apposed nuclear envelopes [11–15]. ELCS have been observed in a wide range of organisms, from protozoa to plants [15], and in numerous lymphomas and leukemias; in granulocytes from individuals with Down syndrome and megaloblastic anemia; and in individuals treated with chemo-

¹ To whom reprint requests should be addressed. Fax: (207) 883-1527. E-mail: dolins@fbr.org.

therapeutic agents [16–19]; summarized in [9]). Normal granulocytes also exhibit ELCS, but in very low amounts (approximately 4%) [9]. Furthermore, granulocytes possess highly condensed chromatin, considerably more extensive than observed in RA-differentiated HL-60. TPA-treated HL-60 reveal essentially no nuclear lobulation or ELCS.

The present study delves more deeply into the kinetics of protein changes in the various RA- and TPA-treated differentiated states of HL-60, and includes comparisons to normal granulocytes. The focus is on changes in the levels of nuclear envelope-associated proteins and chromatin-condensing proteins (i.e., histone H1). A description of the changing levels and modifications of nuclear structural proteins constitutes a first step toward developing an understanding of cellular mechanisms for controlling nuclear shape; in particular, understanding mechanisms of granulocytic nuclear lobulation.

MATERIALS AND METHODS

Cells and chemicals. Most of the experiments in this study used the rapidly differentiating cell line (HL-60/S4) [20], generously provided by Dr. A.C. Sartorelli (Yale University, School of Medicine, New Haven, CT), as previously described [9, 10]. The cells were cultivated in RPMI 1640 medium containing 10% fetal calf serum, with penicillin/streptomycin and glutamine added, at 37°C in a humid incubator purged with 5% CO₂/95% air. Neutrophils were isolated from heparinized venous blood of normal individuals, following well-established procedures [21–24], involving centrifugation in a Ficoll–Hypaque (Amersham Pharmacia Biotech, Inc.) density gradient. Employing this procedure, it is routine to prepare granulocytes with >95% viability and <1% mononuclear cells. RA and TPA were purchased from Sigma Chemical Co. (St. Louis, MO). RA was dissolved in ethanol at a concentration of 1 mmol/L; TPA was dissolved in acetone at a concentration of 160 μmol/L. Both stocks were stored at –20°C. For differentiation, RA was employed at 1 μmol/L; TPA, at 16 nmol/L.

Antibodies. Many of the antibodies to nuclear envelope and cytoskeletal components (e.g., anti-lamins A/C and B2, LAP2β, LBR, α-tubulin, and β-actin) employed in this study have been described previously [9, 10]. Several antibodies were generous gifts: anti-lamin A (mAb 133a2) and anti-lamin B1 (mAb 119D5F1) were from Dr. J. L. V. Broers (Univ. Maastricht, The Netherlands); rabbit anti-H1 subtypes from Drs. M. H. Parseghian (Techniclone Corp., Tustin, CA) and B. A. Hamkalo (Univ. of California, Irvine); rabbit anti-HP1α from Dr. B. Buendia (Univ. of Paris, Jussieu, France); rabbit anti-monoacetylated H4 (Ac16) from Dr. B. M. Turner (Univ. of Birmingham Medical School, United Kingdom). Several antibodies were obtained commercially: mAb anti-emerin (Medac, Hamburg, Germany); anti-phosphorylated H1 (Upstate Biotech., Waltham, MA); mAb anti-NuMA (Transduction Lab., Lexington, KY).

Immunoblotting procedure. Cells (HL-60/S4 and granulocytes) were counted in a hemocytometer, washed, extracted, electrophoresed, and immunoblotted as described previously [10]. Immunoblots were developed by enhanced chemiluminescence (ECL), and subsequently stained with Coomassie blue. Antibody-reactive protein bands visualized on the exposed films were scanned and quantitated on an AlphaImager densitometer (Alpha Innotech Corp.) using CCD imaging and analysis with appropriate software.

Immunofluorescence and confocal microscopy. For experiments on flattened cell preparations, suspensions of HL-60/S4 cytospun

onto ethanol-cleaned slides, or TPA-treated cells attached to coverslips, were fixed with methanol, acetone, air-dried, and immunostained as described previously [9]. For experiments on cells fixed with 3.7% HCHO and immunostained to preserve 3-D architecture, the method described in [10] was followed. Nonconfocal images were collected on a Zeiss axioplan microscope using a Photometrics Quantix CCD camera controlled by IPLab Spectrum 3.1.1 software. Confocal images were collected on a Leica TCS SP spectral microscope (Leica Microsystems Heidelberg GmbH, Heidelberg, Germany).

Acid extraction of cells and capillary zone electrophoresis (CZE). Usually 5×10^7 cells were centrifuged and washed once with PBS. Perchloric acid (PCA) was added to the washed cell pellets in Eppendorf tubes: 1.5 ml of 5% PCA, vortexed 1 h at RT. The cell suspensions were centrifuged for 30 min at 13,000 rpm and supernatants transferred to 50-ml Corex centrifuge tubes. Cell pellets were extracted twice more with 5% PCA (ca. 1 min of vortexing) and supernatants pooled, and 9 vol of ice-cold acetone was added to the Corex tubes. Following an overnight incubation of the covered tubes at –20°C, samples were centrifuged in a swinging bucket rotor (10,000 rpm, 30 min, 4°C), and pellets were washed and centrifuged twice (10,000 rpm, 15 min, 4°C) in ice-cold acetone and air-dried. Prior to CZE analysis, the dried pellets were dissolved in 70 μL of 30 mM HCl (shaking for 30 min at 37°C) and centrifuged to remove any residual precipitates. CZE of the acid extracts was performed as previously described [25–27] on a Perkin–Elmer/Applied Biosystems 270A-HT system. Following sample injection, absorbance at 200 nm was recorded to measure retention time for each peak. Analysis of the relative amount of each peak (expressed as percentage of each H1 subtype within the total acid extract) was performed with computer-aided baseline subtraction and integration. Absolute absorbance varied with total protein loaded on the CZE.

RESULTS

Changes in Expression Levels and Cellular Localization of Nuclear Envelope-Associated Proteins during Differentiation of HL-60/S4 by RA and TPA

Immunoblotting experiments were performed on extracts made daily of unsynchronized cultures of HL-60/S4 exposed to RA or TPA for up to 5 days, using antibodies to various nuclear envelope components. In order to achieve a more quantitative comparison of the relative amounts of selected proteins, cells were counted prior to preparation of extracts. Different electrophoretic lanes were loaded with extracts from identical numbers of cells. After electrophoretic transfer onto PVDF membranes, Ponceau S staining demonstrated that the protein loads in different lanes were comparable, which was reconfirmed by Coomassie blue staining of the membranes following the immune reaction and ECL.

RA and TPA promoted very different changes in cell titer and morphology, as described earlier [9, 10, 20, 28, 29]. RA-treated HL-60/S4 remained in suspension, increasing their cell titer sixfold by Day 5. Specifically, titers increased twofold after 1 day of drug treatment, another twofold between Days 1 and 2, and approximately 50% between Days 2 and 3, with no further increases on Days 4 and 5. Thus, it appears that the

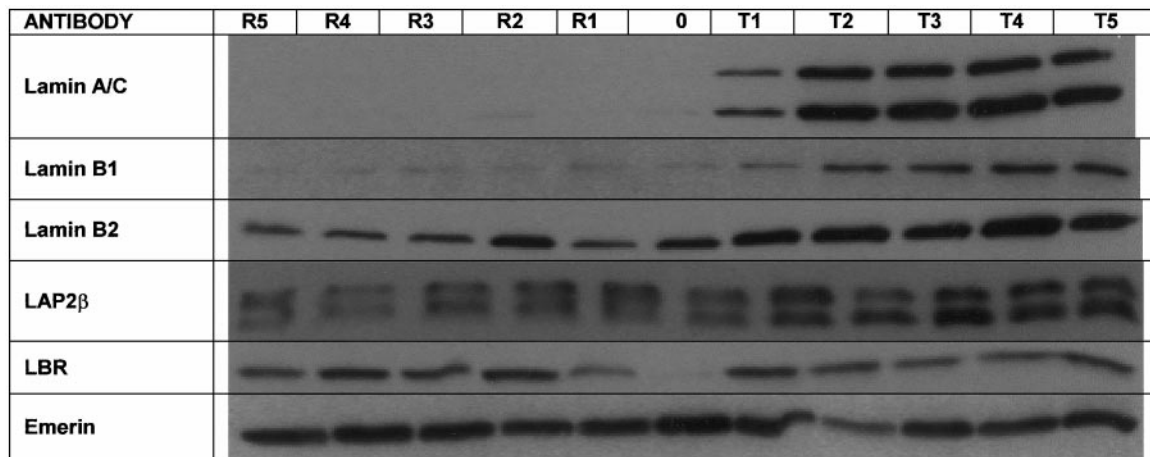


FIG. 1. Immunoblots of nuclear envelope components in undifferentiated and RA- and TPA-treated HL-60/S4. Total cell extracts from the same number of cells were loaded on each gel lane. Cells were harvested on a daily basis: 0, undifferentiated; R1–R5, RA treatment for 1–5 days; T1–T5, TPA treatment for 1–5 days. Specific primary antibodies employed: lamin A/C, mAb R27; lamin B1, mAb 119D5F1; lamin B2, mAb x223; LAP2 β , mAb 6G11; LBR, affinity-pure rabbit anti-LBR; emerlin, mAb anti-emerin.

undifferentiated HL-60/S4, exposed to RA, undergoes slightly more than two division cycles before achieving a growth plateau by Day 3. Parallel microscopic observation on Wright–Giemsa-stained cytopun preparations of RA-treated HL-60/S4 [9] indicated that nuclear lobulation is observed by Day 3, maximal by Days 4 and 5, after which apoptosis begins its appearance. Comparative data [20] on RA-treated HL-60/S4 indicated that: (1) approximately 90% of cells are positive for NBT reduction by Day 4; (2) approximately 60% of cells exhibit phagocytic activity by Day 5. TPA-treated HL-60/S4 cells, on the other hand, attach to glass or plastic substrates by the end of Day 1, many spreading out with flattened ovoid nuclei that never exhibit lobulation, others forming clumps of cells with ovoid nuclei. It is necessary to scrape the TPA-treated cells prior to measuring cell titer and performing extractions. Cell titers never increased more than ca. 25% during the 5-day exposure to TPA, suggesting that cell division ceases rapidly.

Figure 1 displays examples of immunoblots of total protein extracts from HL-60/S4 (treated for up to 5 days with RA or TPA) tested with various antibodies against nuclear envelope components (for recent reviews of these components, see [30, 31]). A summary of semiquantitative observations from these immunoblots (and others, discussed later) are presented in Table 1. Previous studies from our laboratory [9, 10] indicated that during RA-induced differentiation of HL-60/S4: (1) lamins A/C decreased slightly from their very low level in undifferentiated cells; (2) lamin B2 and LAP2 β remained essentially unchanged; (3) lamin B receptor (LBR) increased approximately three- to fourfold.

The present study confirms these observations and

extends them to other nuclear envelope components, and to TPA-induced differentiation. For several of the immunoblots shown in Fig. 1, band intensities were measured and ratios of increase (or decrease) were estimated, compared to the undifferentiated state. Ratios are expressed as average relative changes for the period of peak differentiation (i.e., RA, Days 3–5; TPA,

TABLE 1
Changes in the Level of Various Proteins during HL-60/S4 Cell Differentiation

Protein	0 ^a	RA ^b	TPA ^b
Lamin A, C	Trace	-- ^c	+++
Lamin B1	Weak	–	++
Lamin B2	Strong	nc	+
LAP2 β	Moderate	nc	nc
LBR	Weak	+++	+++
Emerin	Strong	nc	nc
HP1 α	Moderate	+	+
H1 (total)	Strong	nc	nc
H1.5	Strong	nc	nc
H1.3	Not detectable	nc	nc
Phospho H1	Not detectable	nc	nc
H4 Ac16	Moderate	---	---
NuMA	Moderate	–	nc
β -Actin	Moderate	++	++
α -Tubulin	Strong	nc	nc
Vimentin	Weak	---	+++

Note. Gel lanes were loaded with extracts from equivalent numbers of cells. 0, undifferentiated; RA, retinoic acid-treated; TPA, phorbol ester-treated.

^a Immunoblotting reaction intensity.

^b Change of intensity during 5 day period.

^c Symbols for changes: +++, significant increase; ++, increase; +, slight increase; nc, no change; –, slight decrease; --, decrease; ---, significant decrease.

Days 2–5). Following TPA treatment, lamins A/C revealed a significant increase in cellular content by Day 1. The average increase for lamin A was 7.5-fold; for lamin C, 10.8-fold. The TPA-induced increase in lamins A/C has been previously observed [32]. By distinguishing between lamins B1 and B2, it could be demonstrated that: (1) the cellular levels of B2 remained largely unchanged (or slightly decreased) during RA treatment, while increasing slightly (10–20%) following TPA; (2) B1 was present in low amounts in undifferentiated and RA treated cells, increasing significantly (3.4-fold) after addition of TPA. Importantly, LBR measurements revealed a rapid increase in cellular content following both RA (3.8-fold) and TPA treatment (3.3-fold), compared to the low levels in undifferentiated cells. LAP2 β , on the other hand, showed very little change in cellular levels under all conditions. In view of the low levels of lamins A/C in the myeloid forms of HL-60/S4 and the recent evidence for interactions between these lamins and emerlin (reviewed in [30, 31, 33]), it was of interest to observe that the cellular levels of emerlin did not reveal major changes following RA and TPA treatment (see later). In summary, the immunoblotting studies clearly indicate that, from the point of view of the components of the nuclear envelope, HL-60/S4 reveals distinct differences comparing the undifferentiated and RA- and TPA-treated differentiation states. TPA-induced cells contain higher amounts of lamins A/C, B1 (possibly, B2) and of LBR, than present within undifferentiated cells. With the exception of LBR, TPA-treated HL-60/S4 cells displayed higher amounts of these nuclear envelope proteins, compared to RA-treated cells.

Previous immunofluorescent and confocal studies [9, 10] documented that the nuclei of RA-treated HL-60 cells acquire extensive amounts of ELCS, in parallel with nuclear lobulation. Employing antibodies to lamin B2, LBR, and LAP2 β , ELCS appeared as brightly stained regions on the nuclear envelopes of cyospun (flattened) and fixed RA-treated HL-60/S4. Often these brightly staining regions were observed within the clefts of lobulated nuclei, regions relatively devoid of DNA, as indicated by the paucity of DAPI staining. Confocal images [10] of fixed suspensions of RA-treated HL-60/S4 presented clear 3-D views of ELCS in relation to the nuclear envelope, supporting the interpretation that the brightly stained regions of cyospun cells are generated by the formation of flattened ELCS.

Immunofluorescent comparisons of cyospun and fixed undifferentiated, and RA- and TPA-treated HL-60/S4 are presented in Fig. 2. Anti-lamin B2 staining revealed a largely uniform distribution of antigen on the nuclear envelope of undifferentiated and TPA-treated cells. RA-treated cells showed brightly stained regions (presumptive ELCS) in the nuclear envelope. Anti-lamin B1 generated weak punctate staining of

nuclear envelopes in undifferentiated and RA-treated cells, and a stronger more uniformly stained envelope in TPA-treated HL-60/S4. Likewise, anti-lamin A yielded clear staining of the envelope in TPA-treated cells, with weaker staining in undifferentiated and RA-treated cells. The immunofluorescent data obtained with anti-lamin antibodies (A and B1) generally agree with the immunoblotting results, supporting that these nuclear envelope components are expressed to a higher extent in TPA-treated HL-60/S4 cells, than in undifferentiated and RA-treated cell states. Immunofluorescent staining with anti-emerlin antibodies demonstrated a clear redistribution of the antigen following differentiation by TPA. Emerlin appeared to be primarily cytoplasmic in undifferentiated and RA-treated HL-60/S4 cells, but localized in the nuclear envelope of TPA-treated cells. The postulated interaction between lamin A and emerlin [30, 31, 33] suggests a basis for the redistribution of emerlin in HL-60/S4: the increased amount of lamin A in TPA-treated cells might furnish the necessary binding sites to attract the high levels of emerlin from the cytoplasm of undifferentiated cells to the nuclear envelope. Thus, HL-60/S4 may prove to be a useful model system to examine the cellular distribution of emerlin, and its relationship to the nuclear envelope and lamin A.

Changes in Subtype Composition of Histone H1 during Differentiation of HL-60/S4 by RA and TPA

The apparent inverse correlation between extensive chromatin condensation and ELCS formation suggests that proteins involved in chromatin condensation may play a role in modulating nuclear envelope deformability. Histone H1 is believed to have a structural role in stabilizing nucleosome higher order structure [34–37]. Human Histone H1 consists of a family of primary amino acid sequence variants (subtypes), denoted H1.1–H1.5, H1⁰ and H1t, which have all been cloned and characterized [38] (for an alternative nomenclature, see [39]). H1t is observed only in the testis; the relative levels of the remaining H1 subtypes exhibit tissue-specific variations [40]. The role of these variations in the levels of H1 subtypes is not entirely clear. However, recent immunoprecipitation studies [41] indicate that transcriptionally active chromatin may possess a different distribution of subtypes, compared to transcriptionally inactive chromatin.

Capillary zone electrophoresis has proven to be a fast, sensitive, and accurate analytical method for measuring the relative amounts of human H1 subtypes [25–27]. In recent studies [26, 27], CZE was employed to examine the changes in relative amounts of H1 subtypes and their phosphorylated forms in a number of human cell lines (including HL-60) induced to undergo apoptosis. It was shown that in HL-60 cells, H1

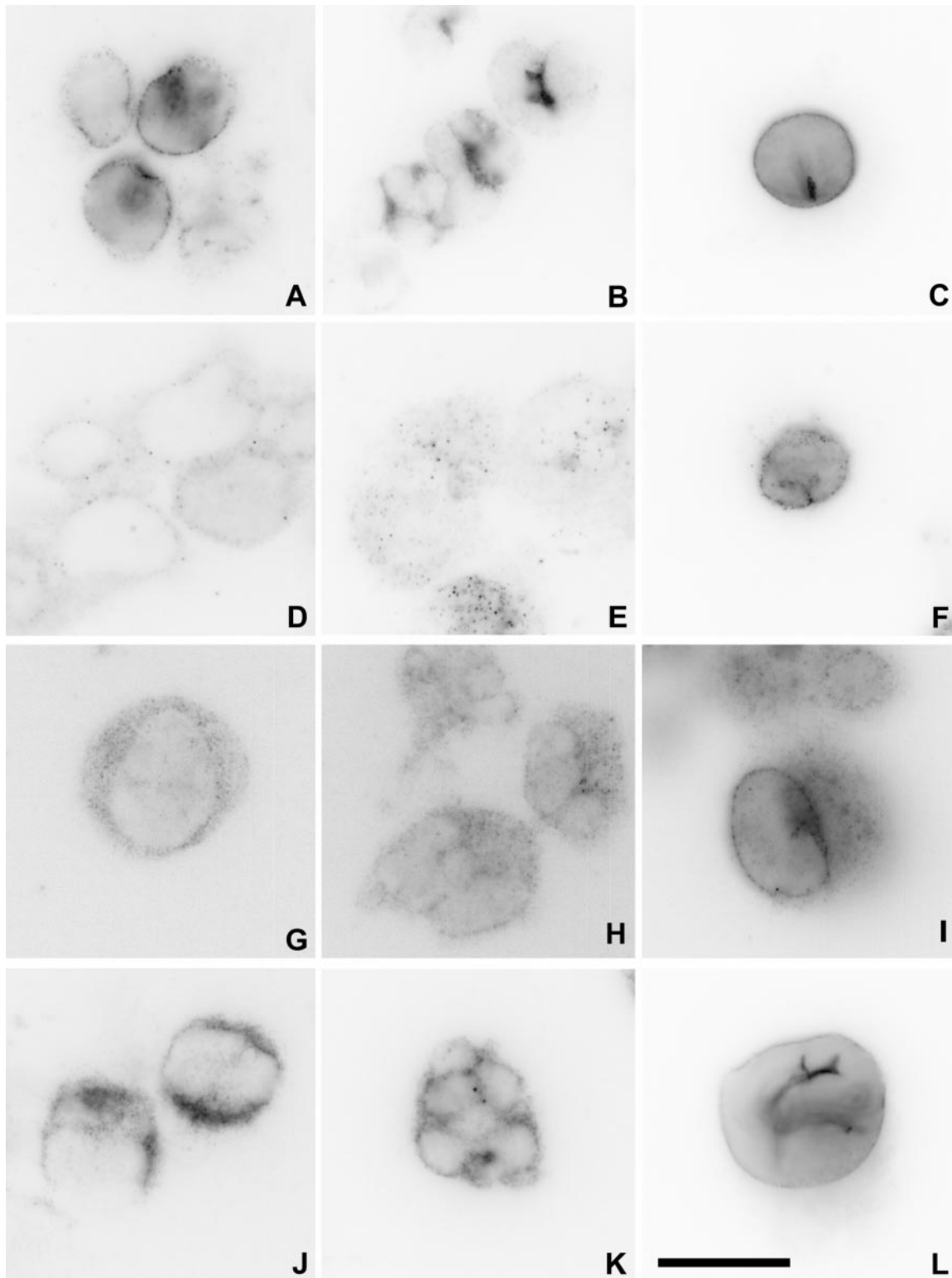


FIG. 2. Immunostaining of nuclear envelope components in undifferentiated and RA- and TPA-treated HL-60/S4. Image contrast is inverted, so that bright fluorescence is black. Columns: A, D, G, J, undifferentiated cells; B, E, H, K, RA-treated 4 days; C, F, I, L, TPA-treated 4 days. Rows: A-C, anti-lamin B2 (mAb x223); D-F, anti-lamin B1 (mAb 119D5F1); G-I, anti-lamin A (mAb 133a2); J-L, anti-emerin. Magnification bar: 20 μ m.

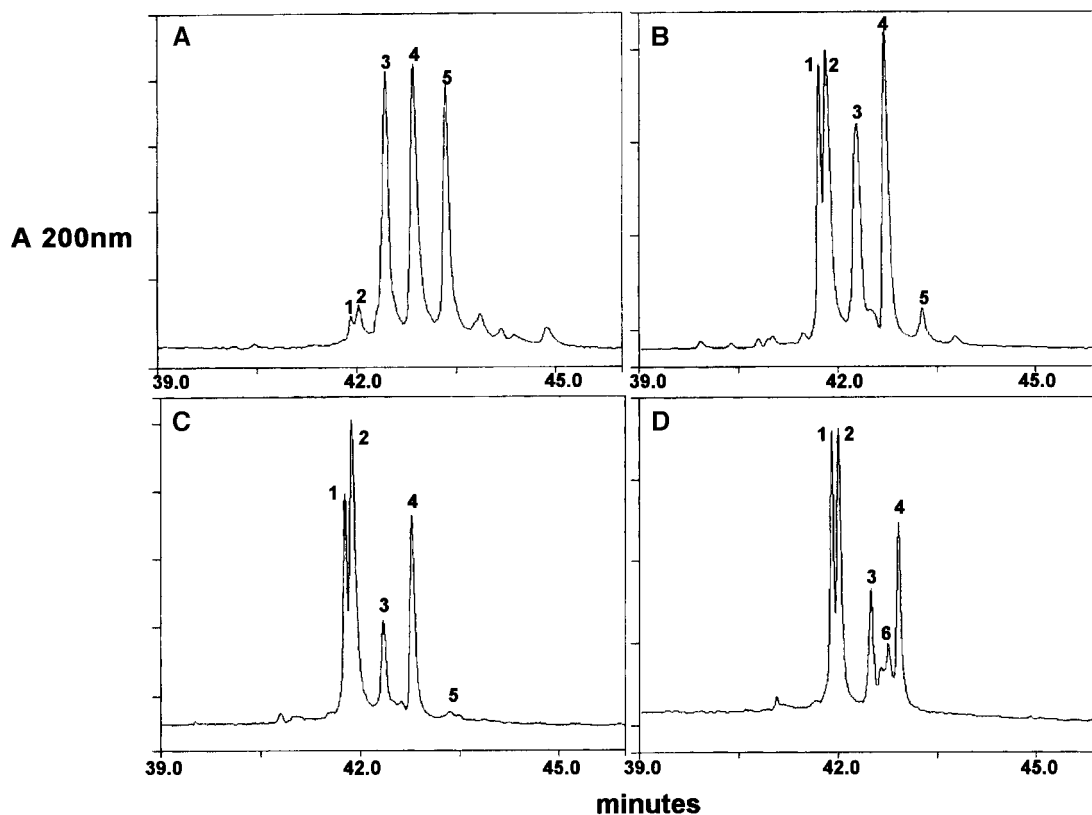


FIG. 3. Protein profiles from capillary zone electrophoresis (CZE) of acid extracts of HL-60/S4 and of granulocytes. (A) Undifferentiated cells; (B) RA-treated 4 days; (C) TPA-treated 4 days; (D) granulocytes. Coordinates: abscissa, absorbance 200 nm; ordinate, retention time (min) following injection of the protein extract. Peak designations: 1, H1.5; 2, H1.4; 3, HMG-17 + 1P H1.4/5; 4, H1.2 + 2P H1.4/5; 5, 1P H1.2 + 3P H1.4/5; 6, H1.3 (where, "*n*P H1.4/5" denotes *n*-phosphorylated forms of H1.4 and H1.5).

histones become rapidly dephosphorylated after induction of apoptosis [27]. The undifferentiated HL-60 cells contained undetectable amounts of H1.1 and H1⁰, rank order of relative amounts being H1.2 > H1.4 > H1.5 > H1.3. Apoptosis resulted in a relative increase in unphosphorylated forms of H1.4 and H1.5. In the present study CZE analysis was performed on acid extracts from undifferentiated and RA- and TPA-treated HL-60/S4 to examine the relative changes in H1 subtypes during the differentiation period for up to 5 days. Representative electrophoresis profiles are presented in Fig. 3. Protein peaks were characterized by retention time (i.e., min after injection of the protein mixture); peaks were identified by adding individual recombinant H1 subtypes to the protein mixture [25, 26]. After subtraction of linear baselines, integrated absorbance values and relative areas for each peak were calculated. Figure 4 presents plots of the daily changes in relative areas for each protein peak in the acid extracts of HL-60/S4. H1⁰, H1.1, and H1.3 were not detected in any extracts of HL-60/S4. For undifferentiated cells, the peaks corresponding to unphosphorylated H1.4 and H1.5 were very low in relative area, increasing significantly by Day 2 of TPA treatment, and Days 3

and 4 of RA treatment. Correspondingly, a few peaks decreased in relative area during the differentiation period, especially a peak that includes monophosphorylated H1.2 and triphosphorylated H1.4 and H1.5. Somewhat less profound is the observed decrease in a peak containing HMG-17 and monophosphorylated H1.2. The overall conclusion from the CZE studies is that H1 subtype modification (i.e., phosphorylation) is significantly reduced during differentiation induced by RA or TPA. The rate of change appears faster (and is more complete) following treatment with TPA, compared to RA-induced differentiation.

The availability of several anti-H1 subtype antibodies [41, 42] permitted an immunoblotting comparison to the data obtained by CZE. Of particular interest were the results obtained with rabbit anti-H1.5 and anti-H1.3 (alternatively designated anti-H1-3 and anti-H1-2 [39], respectively), shown in Fig. 5. These immunoblots demonstrate a relative constancy in the amount of H1.5, comparing undifferentiated, RA- and TPA-treated HL-60/S4. These data support the conclusion (from CZE) that the apparent increase of H1.5 (and probably of H1.4) is due to dephosphorylation during differentiation. Also confirmed by the immuno-

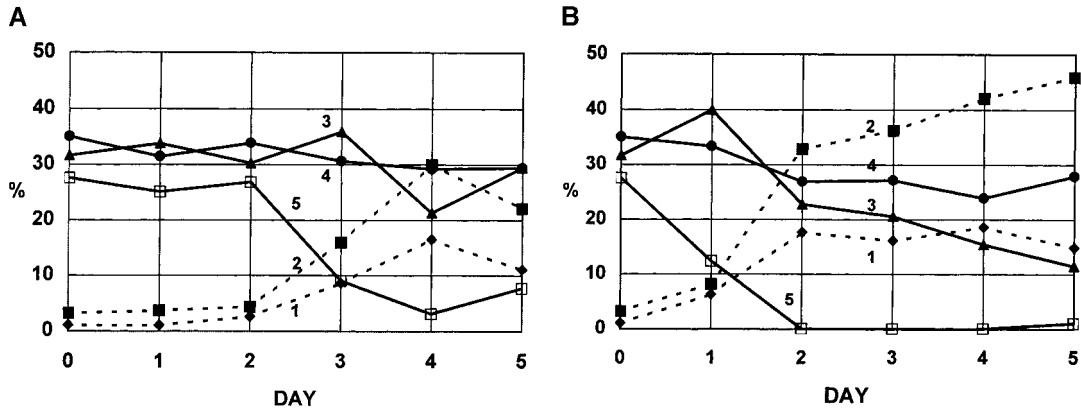


FIG. 4. Daily changes in relative areas of CZE protein peaks from acid extracts of undifferentiated and RA- and TPA-treated HL-60/S4. (A) RA-treated cells; (B) TPA-treated cells. Coordinates: abscissa, % of total absorbance at 200 nm; ordinate, days following addition of RA or TPA. Line designations: 1, H1.5; 2, H1.4; 3, HMG-17 + 1P H1.4/5; 4, H1.2 + 2P H1.4/5; 5, 1P H1.2 + 3P H1.4/5 (where, "nP H1.4/5" denotes n-phosphorylated forms of H1.4 and H1.5).

blot analysis is the negligible amount of H1.3 in all cell states of HL-60/S4. Immunoblots (not shown) were also performed with several monoclonal and polyclonal anti-total H1. The results were very similar to those presented for anti-H1.5; no major changes in H1 levels were observed, comparing undifferentiated and differentiated HL-60/S4. Thus, from the combined CZE and immunoblotting experiments, the only major change observed during RA- or TPA-induced differentiation of HL-60/S4 is the apparent dephosphorylation of the H1 subtypes. This dephosphorylation occurs more rapidly and more completely following TPA, compared to RA, exposure.

Granulocytes Exhibit Similarities and Differences in Histone H1 Subtype and Nuclear Envelope Composition Compared to the Granulocytic Form of HL-60/S4

HL-60 cells are generally employed as an *in vitro* model for granulocytic differentiation; but similarities and differences between the differentiated granulocytic form and normal neutrophils have been noted [1-8]. Extracts were prepared from purified granulocytes of three healthy individuals and examined by CZE and immunoblotting, comparing results with the

undifferentiated and RA- and TPA-differentiated states of HL-60/S4. Figure 3D presents the acid-extract protein profile from the granulocytes of one individual. Two features are apparent: (1) the appearance of a peak, assigned to H1.3, not observed in any cell states of HL-60/S4; (2) elevated levels of H1.4 and H1.5, combined with low relative areas of the peaks containing phosphorylated forms of H1.4, H1.5, and H1.2. Table 2 presents a summary of the relative percentages of the various H1 subtypes in the extracts of granulocytes from the three individuals. Immunoblots with anti-H1.5 and anti-H1.3 (Fig. 5) compare normal granulocytes to the HL-60/S4 cell states, demonstrating the clear presence of H1.3 in granulocytes.

Confocal immunofluorescence studies were performed on normal human granulocytes fixed to preserve 3-D structure (Fig. 6). Propidium iodide staining (following RNase) revealed the thick layer of sublamellar heterochromatin. Anti-total H1 yielded a dense staining throughout the nuclear lobes. Anti-H1.3 yielded a scattered punctate staining. These results are very reminiscent of prior studies [42, 43] employing the same antisera on HeLa and on normal human fibroblasts. Interestingly, the authors [43] report that

TABLE 2

Relative Amounts of H1 Subtypes in PCA Extracts of Human Granulocytes

Individual	H1.5	H1.4	HMG17 & 1P		H1.2 and 2P H1.4/5
			H1.4/5	H1.3	
1 ^a	24.0	29.4	13.1	9.3	20.0
2	25.1	24.2	14.7	9.6	19.8
3	24.0	30.3	13.4	6.9	20.6
Average	24.3	28.3	13.6	8.8	20.1

^a Average of duplicate determinations from the same individual.

ANTIBODY	G	R5	R4	R3	R2	R1	0	T1	T2	T3	T4	T5
H 1.5	[band]	[band]	[band]	[band]	[band]	[band]	[band]	[band]	[band]	[band]	[band]	[band]
H 1.3	[band]	[band]	[band]	[band]	[band]	[band]	[band]	[band]	[band]	[band]	[band]	[band]

FIG. 5. Immunoblots of histone H1 subtypes (H1.5 and H1.3) in undifferentiated and RA- and TPA-treated HL-60/S4, and in granulocytes. Total cell extracts from the same number of cells were loaded on each gel lane for HL-60/S4. Approximately the same amount of total protein was loaded for granulocyte extracts (G), as observed for HL-60/S4 extracts. HL-60/S4 cells were harvested on a daily basis: 0, undifferentiated; R1-R5, RA treatment for 1-5 days; T1-T5, TPA treatment for 1-5 days.

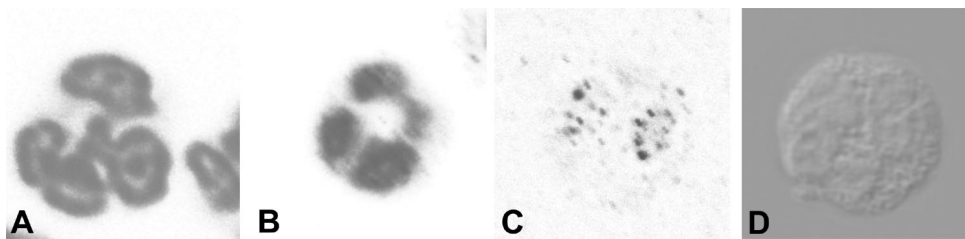


FIG. 6. Confocal slices of stained normal human granulocytes fixed with HCHO to preserve 3-D architecture. (A) Propidium iodide stained following RNase digestion; (B) anti-total H1; (C) anti-H1.3; (D) DIC image of cell in (C).

anti-H1.3 yielded a punctate staining of normal fibroblast nuclei, but (with few exceptions) did not stain HeLa nuclei. The authors suggest that histone H1.3 has a low abundance in HeLa cells, a conclusion confirmed by CZE experiments [25, 26]. It is not clear what is the significance of altered levels of H1.3. Immunoprecipitation studies [41] predict that H1.3 will be found to be concentrated within the heterochromatic chromatin in normal granulocytes.

The protein levels of numerous nuclear envelope and cytoskeletal components in normal granulocytes were determined by immunoblotting (data not shown). Because total extracts from equivalent numbers of HL-60/S4 cells and from granulocytes yielded different amounts of total protein (i.e., granulocytes possessed approximately fourfold less protein/cell than HL-60/S4, as judged by Ponceau S or Coomassie blue staining of the PVDF membranes), it is difficult to make direct comparisons of protein levels between the two cell types. Nonetheless, comparing the results of numerous immunoblots permits several firm conclusions: (1) lamins A/C and B1, LAP2 β , and emerin could not be detected in total granulocyte extracts; (2) lamin B2, LBR, and HP1 α were clearly present; (3) neither phosphorylated histone H1 nor acetylated histone H4 could be detected. In contrast to the previous data on RA-differentiated HL-60/S4 [9, 10], demonstrating an absence of vimentin, granulocyte extracts revealed abundant amounts of vimentin. The presence of vimentin within granulocytes is in agreement with earlier immunolocalization studies [44, 45], demonstrating the accumulation of bundles of vimentin within the uropod of migrating neutrophils.

DISCUSSION

The purpose of the present study is to document the changing levels and modifications of nuclear structural proteins in the HL-60 myeloid leukemic cell line, in order to develop an understanding of cellular mechanisms for controlling nuclear shape; in particular, understanding mechanisms of granulocytic nuclear lobulation. During normal granulopoiesis within human bone marrow, the final postmitotic differentiation

phase (ca. 6.5 days duration) involves significant nuclear structural changes, including lobulation and chromatin condensation [46]. The molecular mechanisms generating these structural changes are largely unknown. A recent review [47] postulates the existence of a chromatin condensing factor, which also promotes tight chromatin–nuclear envelope interactions. Unfortunately, no such factor has been definitively identified, although an interesting candidate might be MENT [48, 49], a 42-kDa chromatin-binding protein, abundant within granulocyte nuclei. However, control of interphase nuclear shape appears to depend upon numerous other factors as well, such as nuclear envelope composition and integrity of cytoskeletal elements [50–55]. In addition, nuclear envelope–centrosome interactions [10, 56, 57] may play a role in influencing nuclear shape. Spermatogenesis probably represents the best documented system of differentiation involving a change of nuclear shape associated with changes in lamin and lamina-associated protein composition and distribution [51, 53, 58], and with chromatin changes, including the appearance of the histone H1t subtype [40, 59].

HL-60 cells furnish a convenient model system for examining the nuclear changes observed during granulopoiesis [1–3]. These robust cells can be grown in large quantity, and can be induced to differentiate *in vitro* into granulocytic or monocytic/macrophage form by the addition of RA or TPA, respectively. Differentiation to either cell state takes only several days, facilitating a detailed comparison of the changes in levels of candidate proteins that might influence or control the nuclear structural changes. Unlike normal peripheral blood granulocytes, RA-treated HL-60 cells exhibit very little condensed chromatin; but reveal extensive amounts of nuclear envelope-limited chromatin sheets [9]. Ultrastructural studies suggested that during RA-induced differentiation of HL-60/S4, nuclear volume decreased and nuclear envelope surface area increased [9]. Studies from this laboratory [9, 10] have attempted to identify candidate proteins that might be key factors in the generation of nuclear lobulation and ELCS formation. The present study provides a detailed account

of changes in nuclear envelope and histone H1 composition among undifferentiated and RA- and TPA-induced HL-60/S4 cells, including a comparison with normal human granulocytes.

The nuclear envelope displays clear differences in composition, comparing undifferentiated and RA- and TPA-treated HL-60/S4 cells (Table 1). Lamins A/C and B1 are largely absent in the undifferentiated and RA treated cells, but clearly expressed after TPA induction. This augmented expression of lamins A/C following phorbol ester treatment has been previously observed [32, 60]. Although not a nuclear envelope component, the changes in vimentin levels during differentiation of HL-60/S4 parallel those seen with lamins A/C and B1, in agreement with prior observations [9, 10, 60]. Whereas the present study is in agreement with an earlier publication [60] on the increased levels of lamins A/C and vimentin following TPA treatment of HL-60, there is disagreement with regard to the consequences of granulocytic differentiation. The earlier study induced differentiation of HL-60 with DMSO and reported an increase of lamins A/C and vimentin; the opposite of the present observations following RA treatment of HL-60/S4. Comparison of light micrographs in [9] and [60] suggests that granulocytic differentiation is more complete following RA, compared to DMSO induction. Other experimental differences that might contribute to the divergent conclusions are the specific cell lines employed, and the analysis of Triton X-100-resistant residual fraction [60] versus analysis of total cell extracts [9, 10, present study].

Several nuclear envelope components (i.e., lamin B2, LAP2 β , and emerin) do not appear to change greatly in amount during either RA- or TPA-induced differentiation. Immunofluorescent studies revealed that both lamin B2 and LAP2 β remained localized to the nuclear envelope in undifferentiated and RA- and TPA-treated HL-60/S4. Furthermore, immunofluorescent and immunoelectron microscopic studies [9] demonstrated that lamin B2 and LAP2 β colocalize in ELCS. However, present immunofluorescent studies show that emerin is largely cytoplasmic in undifferentiated and RA-treated cells, but clearly associated with the nuclear envelope following TPA. Considerable recent attention has been paid to emerin mutations (reviewed in [30, 31, 33]) and its role in the pathogenesis of the Emery–Dreifuss muscular dystrophy (EDMD) phenotype. One postulated mechanism is that emerin–lamin A interactions serve to stabilize the nuclear envelope against mechanical stresses, which are expected to be more recurrent in muscle cells. Mutations in either partner might disrupt the complex, weakening the nuclear envelope. In a recent study [61], myoblasts (which contain lamin A/C) were transfected with GFP–emerin mutant constructs. Some constructs localized emerin

within the nuclear envelope, some within the cytoplasm, permitting an analysis of emerin functional domains. As a test for the postulated mechanism of EDMD, a mouse knockout mutant for lamin A has been created [62]. The null mouse displays many characteristics of EDMD. Of particular interest to the present study, ultrastructural data demonstrated that peripheral (i.e., sublaminar) heterochromatin is considerably disrupted and almost absent. Clearly, this is not the case either for the granulocytic form of HL-60/S4 [9] or for neutrophils [46, 47], both of which have negligible amounts of lamin A/C. The increase in lamin B1 in the nuclear envelope of TPA-treated HL-60/S4, along with the increased amount of lamin A/C, is given significance by immunoprecipitation data [61], which revealed interactions between emerin and lamins A/C and B1. The lack of significant increase in amounts of lamin B2 and LAP2 β during RA-induced differentiation combined with the ultrastructural morphometric data [9], demonstrating a significant increase in the amount of nuclear envelope (including ELCS), suggests that these proteins are being diluted on the envelope during the differentiation.

LBR increases significantly from the undifferentiated cell state during both RA- and TPA-induced differentiation. Therefore, increased LBR cannot be the sole factor in promoting nuclear lobulation or ELCS formation. However, the immunofluorescent colocalization of LBR and lamin B2 within ELCS [9] would be consistent with a supportive role of LBR in the formation of ELCS. Following TPA treatment, the increase in LBR is paralleled by an increase of lamin B1, and slight increases in lamin B2. No such parallel occurs after RA treatment, even though LBR increases three- to fourfold [10]. The general view is that there is a direct interaction between LBR and lamin B [30, 31], although *in vitro* evidence [63] does not support this presumption.

Human HP1 α is one isotype of a class of proteins that may be involved in heterochromatin formation and/or stabilization [64]. Evidence has been presented showing that LBR interacts with HP1 α [65], which might stabilize linkage between the nuclear envelope and peripheral heterochromatin. The present immunoblotting data indicated that the levels of HP1 α did not change appreciably even though LBR levels did, comparing undifferentiated or RA- or TPA-treated HL-60/S4. Immunofluorescent studies of RA-induced differentiation (unpublished) did not detect any significant change in nuclear distribution: the staining was punctate throughout nuclei [66]. Thus, nuclear lobulation and formation of ELCS do not appear to be obviously related to HP1 α amount or distribution.

The immunoblotting and CZE evidence in this study argues for, and is consistent with, a general “shutting-down” of chromosomal functions [67, 68] during the

terminal differentiation of HL-60/S4 induced by either RA or TPA. Histone H4 monoacetylation and H1 phosphorylation decrease markedly, compared to the rapidly growing undifferentiated HL-60/S4 cells. The rate of change occurs faster with TPA treatment (complete by Day 2), compared to that of RA-treated cells (complete by Day 4). Evidence for a decrease in nucleolar function during DMSO-induced granulocytic differentiation has been provided [69], documented by reduced levels of topoisomerase II, B23/nucleophosmin/NO-38, and poly(ADP-ribose) polymerase. However, not all genes are down-regulated during granulocytic differentiation of HL-60; e.g., caspases 1 and 3 exhibit increased levels of expression [70].

The nuclear protein NuMA is a component of the interphase nuclear matrix and associates with the spindle poles during mitosis [71]. It appears to be absent from the nuclei of sperm cells and peripheral blood granulocytes [72]. Based upon these and other findings, the authors suggest that "NuMA may . . . be involved in defining the nuclear shape in interphase cells and that the absence of NuMA may allow the cell to modulate the nuclear architecture. . ." [72]. The present immunoblotting data indicated that the levels of NuMA did not change appreciably, comparing undifferentiated or RA- or TPA-treated HL-60/S4. Thus, in this cell system, nuclear lobulation and formation of ELCS do not appear to be obviously related to the amount of NuMA.

From the point of view of the present study, the major biochemical characteristics of the granulocyte nucleus are the paucity of nuclear envelope components and the extensive amount of peripheral heterochromatin. The nuclear envelope contains detectable amounts of lamin B2 and LBR, but negligible amounts of lamins A/C and B1, LAP2 β , and emerin. The paucity of nuclear envelope components raises the question of what factors maintain the integrity of the neutrophil nucleus, especially when the nuclear lobes are pushed around during cell migration [28]. Perhaps the thickened sublaminar heterochromatin behaves as a stabilizing structural element, also inhibiting the formation of ELCS. So far, the mechanism of granulocytic chromatin condensation is not understood. Candidates for condensation include MENT [48, 49] and increased levels of histone H1.3 subtype, in concert with histone H4 deacetylation and H1 dephosphorylation. Chromatin condensation is a feature of nuclei undergoing apoptosis, which is also accompanied by massive histone H1 dephosphorylation [27]. Recent studies [73, 74] have demonstrated that histone H1 is dynamically associated with chromatin, becoming more immobile when dephosphorylated. Such data suggest that chromatin conformational states within granulocyte (and differentiating HL-60/S4 cells) become more stabilized during H1 dephosphorylation. Another candidate for

nuclear envelope stabilization and inhibition of ELCS might be sufficient levels of vimentin, as observed in granulocytes and TPA-treated HL-60/S4, but not in the granulocytic form of HL-60/S4. Suggestions that lamin polymers within interphase nucleoplasm might constitute a nucleoskeletal framework connected to the lamina [75] and references therein) are of interest, but remain to be established. Clearly, if such a framework exists, the paucity of lamins in granulocytic cells might constitute an additional basis for nuclear deformability.

HL-60 cells exhibit differentiation when treated with a variety of chemical agents, some "physiological" (e.g., RA and vitamin D3) and some "nonphysiological" (e.g., DMSO and TPA). A study of monocyte/macrophage development induced with vitamin D3 [76] documented that differentiation (i.e., expression of CD11b cell surface marker and a macrophage-specific esterase) can occur before cell division ceases. Clearly, it would be of considerable importance for future studies to explore the nuclear envelope and chromatin compositional changes in HL-60/S4 cells induced to monocyte/macrophage differentiation with vitamin D3. Such data, compared with the present information on TPA-treated HL-60/S4 cells, might dissect those nuclear envelope and chromatin changes associated with cessation of proliferation from those associated with monocyte/macrophage differentiation.

As mentioned earlier, there are both similarities and differences between the *in vitro* chemically induced granulocytic differentiation of HL-60 cells and normal granulopoiesis [1–8]. Differences have been observed with regard to the synthesis of proteins within neutrophil specific granules [8, 77]. In terms of nuclear structure, our laboratory has observed several clear differences ([9, 10] and the present study): (1) extensive condensed chromatin in neutrophils versus very little in RA-treated HL-60 cells; (2) profuse amounts of ELCS in RA-treated HL-60 versus only trace amounts in normal granulocytes; (3) presence of subtype H1.3 in neutrophils versus negligible amounts in RA-induced granulocytes; (4) negligible levels of emerin and LAP2 β in granulocytes versus significant levels in RA-treated HL-60 cells. Another difference noted in the present study is the negligible amount of vimentin in RA-treated HL-60/S4 versus its presence in peripheral blood granulocytes. Such differences add a note of caution to formulating models of normal granulopoietic processes from *in vitro* leukemic cell systems, a point made earlier [77].

It is useful to develop a working hypothesis of normal granulocytic nuclear lobulation, based upon the available data from differentiating HL-60 cells. (1) Normal myeloid progenitor cells of the bone marrow are assumed to have low amounts of lamins A/C and B1 (by analogy with the undifferentiated form of HL-60/S4), possessing a more deformable interphase nuclear

envelope compared to most cells. (2) In the appropriate microenvironment, normal progenitor cells are induced to differentiate to granulocytes, chromatin condensation factors are expressed leading to the formation of peripheral heterochromatin, the nuclear surface area/volume increases, and the nuclear envelope remains highly deformable. (3) Under different conditions, normal progenitor cells are induced to differentiate toward the monocyte/macrophage direction. By analogy with TPA-treated HL-60/S4 cells, the working hypothesis assumes an enhanced expression of lamins A/C and B1, and incorporation of emerin into the nuclear envelope, resulting in an increased envelope stability. Since nuclear lobulation does not occur in the monocyte/macrophage lineage, the hypothesis postulates that the nuclear surface area/volume does not increase significantly. With both directions of differentiation (i.e., granulocyte or monocyte/macrophage), increased amounts of LBR are anticipated, reflecting an increased amount of nuclear envelope-associated heterochromatin. Comparison of the differentiating HL-60 cells with normal granulocytes suggests that nuclear lobulation can occur in the absence of extensive amounts of condensed chromatin and of vimentin, and is not an inevitable consequence of increased amounts of LBR, of histone H4 deacetylation, or of H1 dephosphorylation. The HL-60 cell system offers the possibility to test these conclusions by modulating levels of candidate factors with transfection experiments, monitoring effects on RA-induced nuclear lobulation, ELCS formation, and chromatin condensation. Ultimately, this working hypothesis must be examined in the light of data on the granulopoiesis of normal human hematopoietic progenitor cells.

The authors express their appreciation to the scientists (mentioned under Materials and Methods) who provided us with antibodies. A.L.O. and D.E.O. were supported by Guest Scientist fellowships from the German Cancer Research Center; H. H. by the Förderprogramm der Gemeinsamen Forschungskommission der Medizinischen Fakultät Heidelberg; P.L. by a grant (01KW9620) from BMBF "Förderkonzept Humangenomforschung." M.K. and D.D. were supported by the Deutsche Forschungsgemeinschaft (Do 143/19-1).

REFERENCES

- Collins, S. J. (1987). The HL-60 promyelocytic leukemia cell line: Proliferation, differentiation, and cellular oncogene expression. *Blood* **70**, 1233–1244.
- Breitman, T. R. (1990). Growth and differentiation of human myeloid leukemia cell line H-60. In "Methods in Enzymology" (L. Packer, Ed.), Vol. 190, pp. 118–130, Academic Press, New York.
- Yen, A. (1990). HL-60 cells as a model of growth control and differentiation: The significance of variant cells. *Hematol. Rev.* **4**, 5–46.
- Brackmann, D., Lund-Johanson, F., and Aarskog, D. (1995). Expression of cell surface antigens during the differentiation of HL-60 cells induced by 1,25-dihydroxyvitamin D₃, retinoic acid and DMSO. *Leuk. Res.* **19**, 57–64.
- Savill, J. S., Wyllie, A. H., Henson, J. E., Walport, M. J., Henson, P. M., and Haslett, C. (1989). Macrophage phagocytosis of aging neutrophils in inflammation: Programmed cell death in the neutrophil leads to its recognition by macrophages. *J. Clin. Invest.* **83**, 865–875.
- Martin, S. J., Bradley, J. G., and Cotter, T. G. (1990). HL-60 cells induced to differentiate towards neutrophils subsequently die via apoptosis. *Clin. Exp. Immunol.* **79**, 448–453.
- Solary, E., Bertrand, R., and Pommier, Y. (1994). Apoptosis of human leukemic HL-60 cells induced to differentiate by phorbol ester treatment. *Leukemia* **8**, 792–797.
- Le Cabec, V., Calafat, J., and Borregaard, N. (1997). Sorting of the specific granule protein, NGAL, during granulocytic maturation of HL-60 cells. *Blood* **89**, 2113–2121.
- Olins, A. L., Buendia, B., Herrmann, H., Lichter, P., and Olins, D. E. (1998). Retinoic acid induction of nuclear envelope-limited chromatin sheets in HL-60. *Exp. Cell Res.* **245**, 91–104.
- Olins, A. L., Herrmann, H., Lichter, P., and Olins, D. E. (2000). Retinoic acid differentiation of HL-60 cells promotes cytoskeletal polarization. *Exp. Cell Res.* **254**, 130–142.
- Davies, H. G., and Tooze, J. (1964). Electron microscope observations on mitotic chromosomes in erythroblasts of the newt *Triturus cristatus*. *Nature* **203**, 990–992.
- Davies, H. G., and Tooze, J. (1966). Electron- and light-microscope observations on the spleen of the newt *Triturus cristatus*: The surface topography of the mitotic chromosomes. *J. Cell Sci.* **1**, 331–350.
- Davies, H. G. (1968). Electron-microscope observations on the organization of heterochromatin in certain cells. *J. Cell Sci.* **3**, 129–150.
- Haynes, M. E., and Davies, H. G. (1973). Observations on the origin and significance of the nuclear envelope-limited monolayers of chromatin unit threads associated with the cell nucleus. *J. Cell Sci.* **13**, 139–171.
- Davies, H. G., and Haynes, M. E. (1975). Light- and electron-microscope observations on certain leukocytes in a teleost fish and a comparison of the envelope-limited monolayers of chromatin structural units in different species. *J. Cell Sci.* **17**, 263–285.
- Senoo, A., Fuse, Y., and Ghadially, F. N. (1984). A serial section study of nuclear pockets and loops. *J. Submicrosc. Cytol.* **16**, 379–386.
- Ghadially, F. N., Senoo, A., and Fuse, Y. (1985). A serial section study of nuclear pockets containing nuclear material. *J. Submicrosc. Cytol.* **17**, 687–694.
- Bunting, R. W., Selig, M. K., and Dickersin, G. R. (1996). Ultrastructure of peripheral blood granulocytes from patients with low serum cobalamin. *J. Submicrosc. Cytol. Path.* **28**, 187–195.
- Miyauchi, J., Ohyashiki, K., Inatomi, Y., and Toyama, K. (1997). Neutrophil secondary-granule deficiency as a hallmark of all-trans retinoic acid-induced differentiation of acute promyelocytic leukemia cells. *Blood* **90**, 803–813.
- Leung, M.-F., Sokolowski, J. A., and Sartorelli, A. C. (1992). Changes in microtubules, microtubule-associated proteins, and intermediate filaments during the differentiation of HL-60 leukemia cells. *Cancer Res.* **52**, 949–954.
- Hsieh, S.-C., Huang, M.-H., Tsai, C.-Y., Tsai, Y.-Y., Tsai, S.-T., Sun, K.-H., Yu, H.-S., Han, S.-H., and Yu, C.-L. (1997). The expression of genes modulating programmed cell death in normal human polymorphonuclear neutrophils. *Biochem. Biophys. Res. Commun.* **233**, 700–706.

22. Kasahara, Y., Iwai, K., Yachie, A., Ohta, K., Konno, A., Seki, H., Miyawaki, T., and Taniguchi, N. (1997). Involvement of reactive oxygen intermediates in spontaneous and CD95(Fas/APO-1)-mediated apoptosis of neutrophils. *Blood* **89**, 1748–1753.
23. Girard, D., Paquet, M.-E., Paquin, R., and Beaulieu, A. D. (1996). Differential effects of interleukin-15 (IL-15) and IL-2 on human neutrophils: modulation of phagocytosis, cytoskeleton rearrangement, gene expression, and apoptosis by IL-15. *Blood* **88**, 3176–3184.
24. Larochelle, B., Flamand, L., Gourde, P., Beauchamp, D., and Gosselin, J. (1998). Epstein-Barr virus infects and induces apoptosis in human neutrophils. *Blood* **92**, 291–299.
25. Albig, W., Runge, D. M., Kratzmeier, M., and Doenecke, D. (1998). Heterologous expression of human H1 histones in yeast. *FEBS Lett.* **435**, 245–250.
26. Kratzmeier, M., Albig, W., Meergans, T., and Doenecke, D. (1999). Changes in the protein pattern of H1 histones associated with apoptotic DNA fragmentation. *Biochem. J.* **337**, 319–327.
27. Kratzmeier, M., Albig, W., Hanecke, K., and Doenecke, D. (2000). Rapid dephosphorylation of H1 histones after apoptosis induction. *J. Biol. Chem.* **275**, 30478–30486.
28. Campbell, M. S., Lovell, M. A., and Gorbisky, G. J. (1995). Stability of nuclear segments in neutrophils and evidence against a role of microfilaments or microtubules in their genesis during differentiation of HL-60 myelocytes. *J. Leukocyte Biol.* **58**, 659–666.
29. Rovera, G., Santoli, D., and Damsky, C. (1979). Human promyelocytic leukemia cells in culture differentiate into macrophage-like cells when treated with phorbol diester. *Proc. Natl. Acad. Sci. USA* **76**, 2779–2783.
30. Gruenbaum, Y., Wilson, K. L., Harel, A., Goldberg, M., and Cohen, M. (2000). Nuclear lamins—structural proteins with fundamental functions. *J. Struct. Biol.* **129**, 313–323.
31. Dechat, T., Vlcek, S., and Foisner, R. (2000). Lamina-associated polypeptide 2 isoforms and related proteins in cell cycle-dependent nuclear structure dynamics. *J. Struct. Biol.* **129**, 335–345.
32. Kaufmann, S. H. (1992). Expression of nuclear envelope lamins A and C in human myeloid leukemias. *Cancer Res.* **52**, 2847–2853.
33. Wilson, K. L. (2000). The nuclear envelope, muscular dystrophy and gene expression. *Trends Cell Biol.* **10**, 125–129.
34. Widom, J. (1998). Chromatin structure: Linking structure to function with histone H1. *Curr. Biol.* **8**, R788–R791.
35. Belikov, S., and Karpov, V. (1998). Linker histones: Paradigm lost but questions remain. *FEBS Lett.* **441**, 161–164.
36. Travers, A. (1999). The location of the linker histone on the nucleosome. *Trends Biochem. Sci.* **24**, 4–7.
37. Thomas, J. O. (1999). Histone H1: Location and role. *Curr. Opin. Cell Biol.* **11**, 312–317.
38. Albig, W., Meergans, T., and Doenecke, D. (1997). Characterization of the H1.5 gene completes the set of human H1 subtype genes. *Gene* **184**, 141–148.
39. Parseghian M. H., Henschen, A. H., Krieglstein K. G., and Hamkalo, B. A. (1994). A proposal for a coherent mammalian histone H1 nomenclature correlated with amino acid sequences. *Protein Sci.* **3**, 575–587.
40. Doenecke, D., Albig, W., Bode, C., Drabent, B., Franke, K., Gavenis, K., and Witt, O. Histones: Genetic diversity and tissue-specific gene expression. *Histochem. Cell Biol.* **107**, 1–10.
41. Parseghian, M. H., Newcomb, R. L., Winokur, S. T., and Hamkalo, B. A. (2000). The distribution of somatic H1 subtypes is non-random on active vs. inactive chromatin: Distribution in human fetal fibroblasts. *Chromosome Res.* **8**, 405–424.
42. Parseghian, M. H., Harris, D. A., Rishwain, D. R., and Hamkalo, B. A. (1994). Characterization of a set of antibodies specific for three human histone H1 subtypes. *Chromosoma* **103**, 198–208.
43. Parseghian, M. H., Clark, R. F., Hauser, L. J., Dvorkin, L. J., Harris, D. A., and Hamkalo, B. A. (1993). Fractionation of human H1 subtypes and characterization of a subtype-specific antibody exhibiting non-uniform nuclear staining. *Chromosome Res.* **1**, 127–139.
44. Parysek, L. M., and Eckert, B. S. (1984). Vimentin filaments in spreading, randomly locomoting, and f-met-leu-phe-treated neutrophils. *Cell Tissue Res.* **235**, 557–581.
45. Pryzwansky, K. B., and Merricks, E. P. (1998). Chemotactic peptide-induced changes of intermediate filament organization in neutrophils during granule secretion: Role of cyclic guanosine monophosphate. *Mol. Biol. Cell.* **9**, 2933–2947.
46. Bainton, D. F., Ullyot, J. L., and Farquhar, M. G. (1971). The development of neutrophilic PMN leukocytes in human bone marrow: Origin and content of azurophil and specific granules. *J. Exp. Med.* **134**, 907–933.
47. Sanchez, J. A., and Wangh, L. J. (1999). New insights into the mechanism of nuclear segmentation in human neutrophils. *J. Cell. Biochem.* **73**, 1–10.
48. Grigoryev, S. A., and Woodcock, C. L. (1998). Chromatin structure in granulocytes. A link between tight compaction and accumulation of a heterochromatin-associated protein (MENT). *J. Biol. Chem.* **273**, 3082–3089.
49. Grigoryev, S. A., Bednar, J., and Woodcock, C. L. (1999). MENT, a heterochromatin protein that mediates higher order chromatin folding, is a new serpin family member. *J. Biol. Chem.* **274**, 5626–5636.
50. Georgatos, S. D. (1994). Towards an understanding of nuclear morphogenesis. *J. Cell. Biochem.* **55**, 69–76.
51. Furukawa, K., and Hotta, Y. (1993). cDNA cloning of a germ cell specific lamin B3 from mouse spermatocytes and analysis of its function by ectopic expression in somatic cells. *EMBO J.* **12**, 97–106.
52. Yang, L., Guan, T., and Gerace, L. (1997). Lamin-binding fragment of LAP2 inhibits increase in nuclear volume during the cell cycle and progression into S phase. *J. Cell Biol.* **139**, 1077–1087.
53. Alsheimer, M., Fecher, E., and Benavente, R. (1998). Nuclear envelope remodelling during rat spermiogenesis: Distribution and expression pattern of LAP2/thymopoietins. *J. Cell Sci.* **111**, 2227–2234.
54. Saria, A. J., Lieber, J. G., Nordeen, S. K., and Evans, R. M. (1994). The presence or absence of a vimentin-type intermediate filament network affects the shape of the nucleus in human SW-13 cells. *J. Cell Sci.* **107**, 1593–1607.
55. Theodoropoulos, P. A., Polioudaki, H., Kostaki, O., Derdas, S. P., Georgoulas, V., Dargemont, C., and Georgatos, S. D. (1999). Taxol affects nuclear lamina and pore complex organization and inhibits import of karyophilic proteins into the cell nucleus. *Cancer Res.* **59**, 4625–4633.
56. Bornens, M. (1977). Is the centriole bound to the nuclear membrane? *Nature* **270**, 80–82.
57. Maro, B., and Bornens, M. (1980). The centriole-nucleus association: Effects of cytochalasin B and nocodazole. *Biol. Cell.* **39**, 287–290.
58. Goldman, R. D., Baccetti, B., Collodel, G., Gambera, L., Morretti, E., and Piomboni, P. (1998). Localization of lamins in

- mammalian spermatozoa. *J. Submicrosc. Cytol. Pathol.* **30**, 573–580.
59. Ponte, I., Vidal-Taboada, J. M., and Suau, P. (1998). Evolution of the vertebrate H1 histone class: Evidence for the functional differentiation of the subtypes. *Mol. Biol. Evol.* **15**, 702–708.
 60. Paulin-Levasseur, M., Giese, G., Scherbarth, A., and Traub, P. (1989). Expression of vimentin and nuclear lamins during the *in vitro* differentiation of human promyelocytic leukemia cells HL-60. *Eur. J. Cell Biol.* **50**, 453–461.
 61. Fairley, E. A. L., Kendrick-Jones, J., and Ellis, J. A. (1999). The Emery-Dreifuss muscular dystrophy phenotype arises from the aberrant targeting and binding of emerin at the inner nuclear membrane. *J. Cell Sci.* **112**, 2571–2582.
 62. Sullivan, T., Escalante-Alcande, D., Bhatt, H., Anver, M., Bhat, N., Nagashima, K., Stewart, C. L., and Burke, B. (1999). Loss of A-type lamin expression compromises nuclear integrity leading to muscular dystrophy. *J. Cell Biol.* **147**, 913–919.
 63. Mical, T. I., and Monteiro, M. J. (1998). The role of sequences unique to nuclear intermediate filaments in targeting and assembly of human lamin B: Evidence for lack of interaction of lamin B with its putative receptor. *J. Cell Sci.* **111**, 3471–3485.
 64. Jones, D. O., Cowell, I. G., and Singh, P. B. (2000). Mammalian chromodomain proteins: Their role in genome organization and expression. *BioEssays* **22**, 124–137.
 65. Ye, Q., Barton, R. M., and Worman, H. J. (1998). Nuclear lamin-binding proteins. In "Subcellular Biochemistry" (H. Herrmann and J. R. Harris, Eds.), Vol. 31, pp. 587–610, Plenum Press, New York.
 66. Minc, E., Allory, Y., Worman, H. J., Courvalin, J.-C., and Buendia, B. (1999). Localization and phosphorylation of HP1 proteins during the cell cycle in mammalian cells. *Chromosoma* **108**, 220–234.
 67. Spencer V. A., and Davie, J. R. (1999). Role of covalent modifications of histones in regulating gene expression. *Gene* **240**, 1–12.
 68. Cheung W. L., Briggs, S. D., and Allis, C. D. (2000). Acetylation and chromosomal functions. *Curr. Opin. Cell Biol.* **12**, 326–333.
 69. Kaufmann, S. H., Charron, M., Burke, P. J., and Karp, J. E. (1995). Changes in topoisomerase I levels and localization during myeloid maturation *in vitro* and *in vivo*. *Cancer Res.* **55**, 1255–1260.
 70. Watson, R. W. G., Rotstein, O. D., Prado, J., Bitar, R., Hackam, D., and Marshall, J. C. (1997). Granulocytic differentiation of HL-60 cells results in spontaneous apoptosis mediated by increased caspase expression. *FEBS Lett.* **412**, 603–609.
 71. Harborth, J., and Osborn, M. (1999). Does NuMA have a scaffold function in the interphase nucleus? *Crit. Rev. Euk. Gene Funct.* **9**, 319–328.
 72. Merdes, A., and Cleveland, D. W. (1998). The role of NuMA in the interphase nucleus. *J. Cell Sci.* **111**, 71–79.
 73. Lever, M. A., Th'ng, J. P. H., Sun, X., and Hendzel, M. J. (2000). Rapid exchange of histone H1.1 on chromatin in living cells. *Nature* **408**, 873–876.
 74. Misteli, T., Gunjan, A., Hock, R., Bustin, M., and Brown, D. T. (2000). Dynamic binding of histone H1 to chromatin in living cells. *Nature* **408**, 877–881.
 75. Moir, R. D., Yoon, M., Khuon, S., and Goldman, R. D. (2000). Nuclear lamins A and B1: Different pathways of assembly during nuclear envelope formation in living cells. *J. Cell Biol.* **151**, 1155–1168.
 76. Liu, Q., VanHoy, R. W., Zhou, J. H., Dantzer, R., Freund, G. G., and Kelly, K. W. (1999). Elevated cyclin E levels, inactive retinoblastoma protein, and suppression of the p27 (KIP1) inhibitor characterize early development of promyeloid cells into macrophages. *Mol. Cell. Biol.* **19**, 6229–6239.
 77. Sigurdsson, F., Khanna-Gupta, A., Lawson, N., and Berliner, N. (1997). Control of late neutrophil-specific gene expression: Insights into regulation of myeloid differentiation. *Semin. Hematol.* **34**, 303–310.

Received February 20, 2001

Revised version received May 4, 2001